INTERNATIONAL JOURNAL OF PRECISION ENGINEERING AND MANUFACTURING Vol. 18, No. 4, pp. 575-585 APRIL 2017 / 575

REGULAR PAPER

DOI: 10.1007/s12541-017-0069-5
ISSN 2234-7593 (Print) / 2005-4602 (Online)

Development of a Rotary Clap Mechanism for Positive-Displacement Rotary Pumps: Pump Performance Analysis

Sung-Bo Shim[1,#], Young-Jun Park[2,3], Ju-Seok Nam[4], Su-Chul Kim[5], Jong-Mun Kim[6], and Kyeong-Uk Kim[2]

1 Upland-field Machinery, Research Center, Kyungpook National University, 80, Daehak-ro, Buk-gu, Daegu, 41566, South Korea
2 Department of Biosystems and Biometerials Science and Engineering, Seoul National University, 1 Gwanak-ro, Gwanak-gu, Seoul, 08826, South Korea
3 Research Institute for Agriculture and Life Sciences, Seoul National University, 1 Gwanak-ro, Gwanak-gu, Seoul, 08826, South Korea
4 Department of Biosystems Engineering, Kangwon National University, 1 Kangwondaehak-gil, Chuncheon, Gangwon-do, 24341, South Korea
5 Department of System Reliability, Korea Institute of Machinery and Materials, 1156, Gajeongbuk-ro, Yuseong-gu, Daejeon, 34103, South Korea
6 ClapMC Co., Ltd., 156, Gajeongbuk-ro, Yuseong-gu, Daejeon, 34103, South Korea
Corresponding Author / E-mail: environ80@naver.com, TEL: +82-53-950-7289, FAX: +82-53-950-7847

KEYWORDS: Pump driving torque, Pump efficiency, Pump pressure, Pump slip, Rotary clap pump

We have introduced a novel positive-displacement rotary pump named as rotary clap pump, and analyzed its working principles through a kinematic analysis in the previous study. That study mainly described fundamental design parameters of the rotary clap pump and their inter-relationships. As a follow-up research, this study presents the pump performance of the rotary clap pump such as the pressure, driving torque, and efficiency characteristics using related theories and some basic assumptions. In the pressure analysis, the effect of friction, mass acceleration, piping components, and gravity were considered. The forces acting on the pump components and the driving torque are calculated using vector equations based on the results of the previous study. The volumetric, torque, and overall efficiencies are analyzed by calculating the slip flow and frictional forces caused by fluid viscosity. We also present the conditions that minimize the input power and forces acting on the components. The experimental study for the rotary clap pump including comparison with analysis results is prepared to the follow-up paper.

Manuscript received: July 27, 2016 / Revised: December 19, 2016 / Accepted: December 20, 2016

NOMENCLATURE

ϕ: Absolute angular displacement of the gear, rad
r_c: Crank radius, m
θ_c: Angular displacement of the crank, rad
L: Displacement between pins P_1 and P_2, m
r_{p1}: Radius of pin P_1 with respect to the center of rotor O, m
r_{p2}: Radius of pin P_2 with respect to the center of rotor O, m
θ_{p1}: Angular displacement of vector $\mathbf{OP_1}$, rad
θ_{p2}: Angular displacement of vector $\mathbf{OP_2}$, rad
$\Delta p_{f1\text{-}2}$: Pressure head caused by friction, Pa
ρ: Density of fluid, kg/m^3
$f_{1\text{-}2}$: Friction factor
$l_{1\text{-}2}$: Distance between the two sides of the control volume, m
$D_{1\text{-}2}$: Pipe diameter, m
$Q_{1\text{-}2}$: Flow rate, m^3/sec
$A_{1\text{-}2}$: Pipe's cross-section area, m^2
$\Delta p_{a1\text{-}2}$: Pressure head due to mass acceleration, Pa
$\dot{Q}_{1-2}$: Derivative with respect to the time of flow rate, m^3/sec^2
$\Delta p_{K1\text{-}2}$: Pressure head caused by minor losses, Pa
K: Loss coefficient for pipe components
$\Delta p_{h1\text{-}2}$: Pressure head due to gravity, Pa
p_2-p_1: Total pressure head (differential pressure) of the pipe, Pa
k: Number of control volumes
$\Sigma(p_{k+1,s}\text{-}p_{k,s})$: Total pressure head in the suction lines of the pump, respectively, Pa
$\Sigma(p_{k+1,d}\text{-}p_{k,d})$: Total pressure head in the discharge lines of the pump, respectively, Pa
θ_{re}: Relative angular displacement of the two rotors, θ_{p1} - θ_{p2}, rad

W_j: Width of jaw, m

h: Jaw height, m

N: Number of jaws

r_o: Outer radius of rotor, m

$\dot{\theta}_{p1}$: Angular velocity of vector **OP**$_1$, rad/sec

$\dot{\theta}_{p2}$: Angular velocity of vector **OP**$_2$, rad/sec

$\ddot{\theta}_{p1}$: Angular acceleration of vector **OP**$_1$, rad/sec

$\ddot{\theta}_{p2}$: Angular acceleration of vector **OP**$_2$, rad/sec^2

Z_r: Number of teeth on the fixed internal gear

Z_p: Number of teeth on the gear of shaft link

$\dot{\theta}_c$: Angular velocity of the crank, rad/sec

F_{R1}: Force acting on the rotor 1, N

F_{R2}: Force acting on the rotor 2, N

F_d: Force caused by the discharging pressure, N

F_s: Force caused by the suction pressure, N

T_{OR1}: Torque acting on the rotor 1, N·m

T_{OR2}: Torque acting on the rotor 2, N·m

$\Sigma\mathbf{F}_{SUM}$: Summation of the force vectors acting on the gear and shaft link, N

$\Sigma\mathbf{T}_c$: Summation of the torque vectors acting on the gear and shaft link, N·m

I_{R1}: Moment of inertia for rotor 1, kg·m^2

I_{R2}: Moment of inertia for rotor 2, kg·m^2

T_i: Driving torque about point O

$D_p = D/2\pi$: Displacement per degree, m^3/rad

T_{th}: Theoretical torque, N·m

p: Discharge pressure, Pa

v: Velocity in the direction of the x axis, m/sec

τ: Shear stress on a plane parallel to the xz plane, N/m^2

μ: Coefficient of the fluid viscosity, N·sec/m^2

A: Area of the flat plate, m^2

τ_m: Shear stress at the moving plate located at $y = \delta$, N/m^2

τ_f: Shear stress at the fixed plate located at $y = 0$, N/m^2

l: Length of the plate, m

ΔQ_s: Slip flow of a conventional positive-displacement pump, m^3/sec

Δp: Pressure drop through the passage, Pa

C_s: A dimensionless coefficient

T_v: Viscous torque, N·m

C_d: Coefficient of the viscous drag dependent on the pump geometry

T_f: Pressure-dependent frictional torque, N·m

C_f: Coefficient of friction dependent on the pump geometry

$(Q_{sc1})_{tot}$: Total slip flow between the upper and lower surfaces of jaw 1 and the chamber, m^3/sec

$(Q_{ss1})_{tot}$: Total slip flow between the side surfaces of jaw 1 and the chamber, m^3/sec

Q_{ss1f}: Slip flow between the front side surface of jaw 1 and the chamber, m^3/sec

Q_{ss1b}: Slip flow between the back side surface of jaw 1 and the chamber, m^3/sec

$(Q_{sc2})_{tot}$: Total slip flow between the upper and lower surfaces of jaw 2 and the chamber, m^3/sec

$(Q_{ss2})_{tot}$: Total slip flow between the side surfaces of jaw 2 and the chamber, m^3/sec

$(F'_{sc1})_{tot}$: Total forces at jaw 1 caused by the fluid viscosity between the upper and lower surfaces of jaw 1 and the chamber, N

$(F'_{ss1})_{tot}$: Total forces at jaw 1 caused by fluid viscosity between the side surfaces of jaw 1 and the chamber, N

F'_{ss1f}: Forces at jaw 1 caused by the fluid viscosity between the front side surface of jaw 1 and the chamber, N

F'_{sc1b}: Forces at jaw 1 caused by the fluid viscosity between the back side surface of jaw 1 and the chamber, N

$(F'_{sc2})_{tot}$: Total forces at jaw 2 caused by the fluid viscosity between the upper and lower surfaces of jaw 2 and the chamber, N

$(F'_{ss2})_{tot}$: Total forces at jaw 2 caused by the fluid viscosity between the side surfaces of jaw 2 and the chamber, N

1. Introduction

A rotary clap pump has been developed to convert the positive displacement reciprocating pump actions into a rotary mechanism for the reduction of operational vibration and required power. A previous study[1] presented a kinematic analysis and working principles of the rotary clap pump. The important design parameters and their inter-relationships were also investigated.

We confirmed the kinematic operability of the rotary clap pump through the previous study. Now, the pump performance should be confirmed to ensure functionality of the rotary clap pump. The important factors related to pump performance of a pump device are pressure and flow rate. In a more important system, the efficiency, required power and Net Positive Suction Head (NPSH) specs are added in addition to the pressure and flow rate. These factors are important because they are directly related to economic feasibility and system safety of a pump system. A positive displacement pump generates pressure pulsations, which can cause severe system safety and reliability problems and have a detrimental effect on the NPSH. Therefore, pressure pulsation is also an important factor affecting performance of a positive displacement pump.

Regarding conventional positive displacement pumps, a variety of studies to analyze the pump performance have been introduced.[2-6] The performance analysis for the rotary clap pump, however, has not been conducted. This study was conducted to analyze pump performance of the rotary clap pump. The considered performance parameters were the operating pressure, driving torque, and efficiency. These performance characteristics were analyzed based on related theories and some basic assumptions.

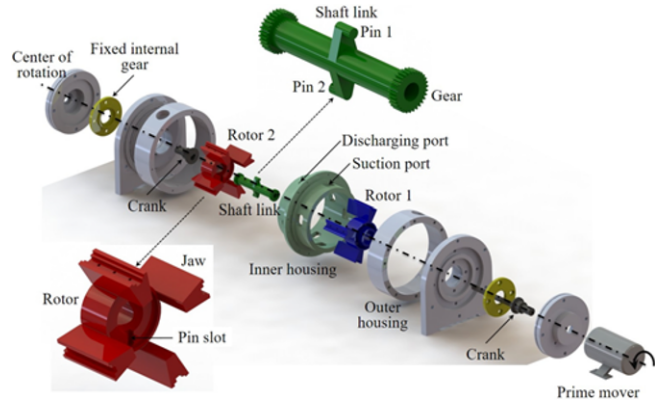

Fig. 1 Structure of rotary clap mechanism as a pumping device (Adapted from Ref. 1 with permission)

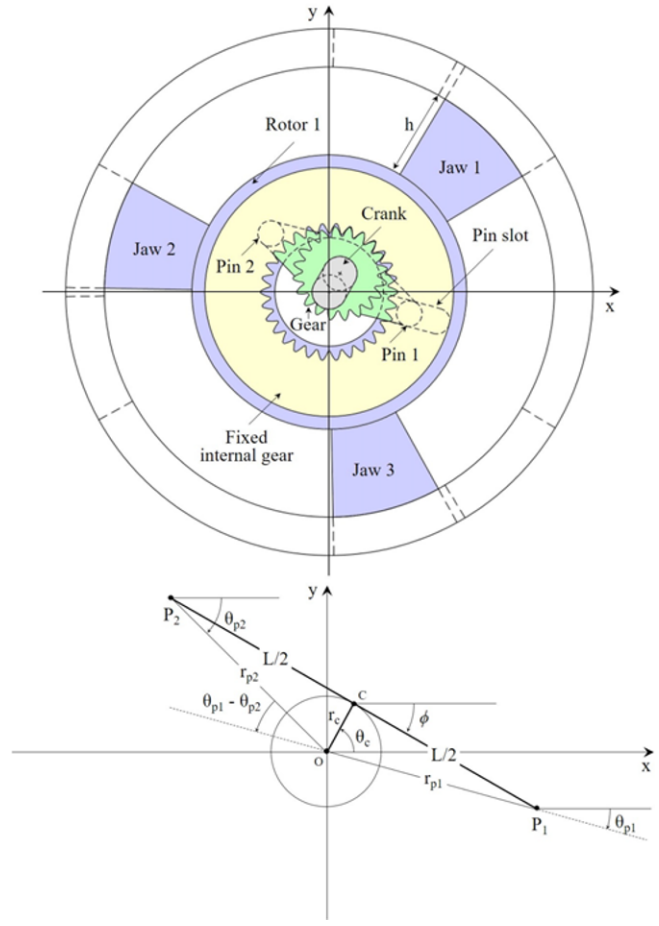

Fig. 2 Motion of the pins relative to the center of rotors (Adapted from Ref. 1 with permission)

2. Overview of the Developed Rotary Clap Pump[1]

The rotational clap mechanism is a five-link spatial mechanism (Figs. 1 and 2) which comprises of a crank as the driving link, a shaft link having two pins symmetrically located in opposite direction at a plate rigidly mounted on its middle and two gears rigidly attached to both ends, two rotors with jaws equally spaced along their circumferences and a fixed internal gear. The width of jaw is extended unilaterally twice of the rotor width so that the two rotors jaws can be engaged completely. As the crank rotates, the gear pin-jointed to the crank rotates around the crank pin and the center of the fixed internal gear at the same time, making the motions of a hypo-cyclic gear train. The shaft link also can rotate around the crank pin and the center of the fixed internal gear at the same time. This motion of the shaft link makes the pins rotate about the center of the fixed internal gear with a periodically-varying radius. The rotors are driven by the pins on the shaft link through a pin-in-slot joint where the pins move along a radial slot on the contacting faces of two rotors. Since the rotational radius of the pin changes as the crank rotates at a constant velocity, angular velocities of the two rotors also change accordingly. The relative velocity between the two rotors makes one rotor lead and lag periodically with respect to the other. These lead and lag motions result in a continuous cycle of approach-contact-recess of two adjacent rotor jaws similar to a hand clapping from which the mechanism is named. The continuous lead and lag motions can be used for the suction and discharge motions required for pumping.[1]

Displacement of the clap mechanism varies with crank radius, pin distance, number of jaws, jaw width and jaw height. It increases with the crank radius at a given number of jaws and pin distance while at a given crank radius it decreases with pin distance and increases with the number of jaws. However, the displacement can be increased as much as possible by increasing the jaw width and height once the crank radius, pin distance and the number of jaws are determined since they are not inter-related with other parameters of the mechanism.[1]

3. Pumping Performance Analysis

3.1 Pressure

We analyzed pressure and its pulsation in this pump on the basis of the following assumptions:

- Incompressible flow.
- Ignoring the elasticity of the piping system.
- Pressure is the same in the control volume.
- Each flow space in the pump is modified with a circular pipe.

3.1.1 Pressure head

Pressure is required to pump liquid through the system for a given flow rate. A sufficiently high pressure is required to overcome the internal resistance of the system, which is also known as the head. The total head is the sum of individual heads as follows:

The pressure head from flow friction in a pipe is given by the well-known Darcy equation.

The pressure head caused by mass acceleration in the control volume of the pipe can be calculated on the basis of Newton's law.[7] The flow in the piping system passes through a variety of components that cause pressure losses, such as nipples, tees, elbows, valves, and orifices. Such losses are generally termed minor losses. The pressure head attributable to gravity should also be considered. Therefore, based on the law of conservation of energy, the differential pressure shown in Fig. 3 can be expressed as the sum of individual heads as shown in Eq. (1).

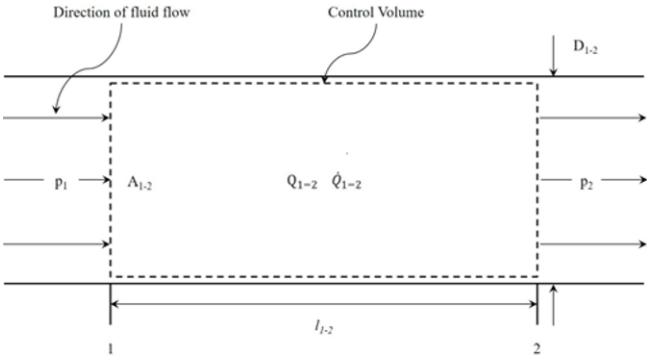

Fig. 3 Fluid flow through a pipe

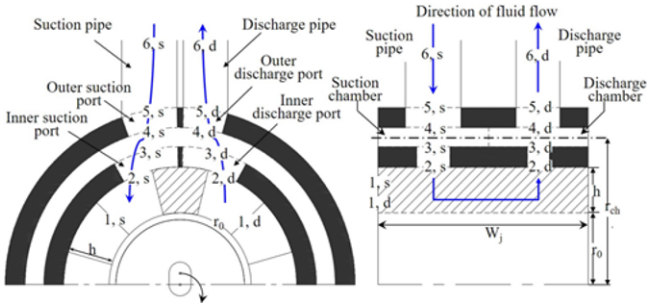

Fig. 4 Fluid movement in the rotary clap pump

$$p_2 - p_1 = \Delta p_{f_{1-2}} + \Delta p_{a_{1-2}} + \Delta p_{K_{1-2}} + \Delta p_{h_{1-2}}$$
$$= \frac{1}{2}\rho \frac{f_{1-2} l_{1-2}}{D_{1-2}} \frac{Q_{1-2}^2}{A_{1-2}^2} + \rho l_{1-2} \frac{\dot{Q}_{1-2}}{A_{1-2}} + \frac{1}{2} K_{1-2} \rho \frac{Q_{1-2}^2}{A_{1-2}^2} \quad (1)$$

3.1.2 Pressure analysis in rotary clap pump

As presented in previous study,[1] the volume variations between two adjacent rotor jaws caused by the hypo-cycle mechanism produce the flow in the pump, as shown in Fig. 4. To apply Eq. (1) to the flow in this pump, we simplified all the suction and discharge spaces in the pump to circular pipes, as shown in Fig. 5. As a result, each of the suction and discharge spaces is divided into five independent control volumes. In other words, in the suction, the space between two adjacent rotor jaws, inner suction port, suction chamber, outer suction port, and suction pipe, respectively, are independent control volumes. In addition, the start points of each control volume are labeled *k, s* (*k: number of control volume*). The spaces of the discharge area are also divided in this manner, and those start points are labeled *k, d*. The space between the two adjacent rotor jaws and that between the inner suction and discharge ports are adjusted based on the number of jaws.[1] However, each space is merged with one of the control volumes. Therefore, the pressure losses in this pump can be expressed as:

$$\Sigma(p_{k+1,s} - p_{k,s}) = \Sigma \frac{1}{2} \rho \frac{f_{k-k+1,s} l_{k-k+1,s}}{D_{k-k+1,s}} \frac{Q_{k-k+1,s}^2}{A_{k-k+1,s}^2}$$
$$+ \rho l_{k-k+1,s} \frac{\dot{Q}_{k-k+1,s}}{\dot{A}_{k-k+1,s}} + \frac{1}{2} \rho \Sigma K_{k-k+1,s} \frac{Q_{k-k+1,s}^2}{A_{k-k+1,s}^2} + \rho g h_{k-k+1,s} \quad (2)$$

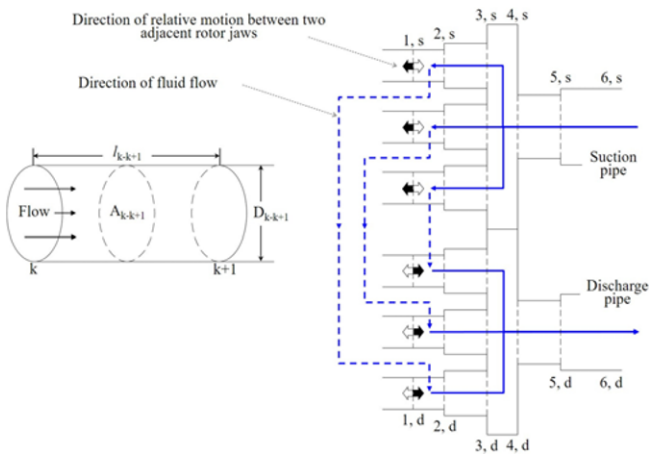

Fig. 5 A schematic diagram of the fluid movement in the rotary clap pump

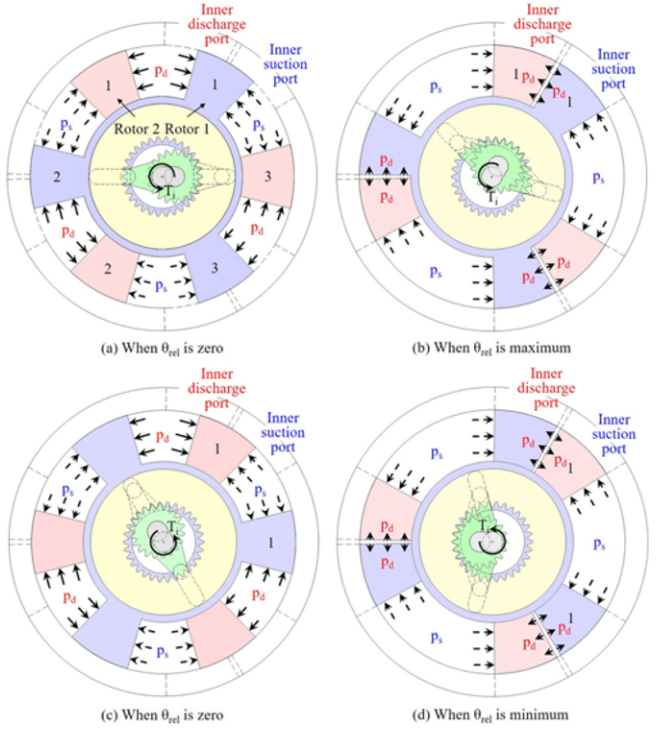

Fig. 6 Direction changes in hydraulic forces acting on the rotors and housing

$$\Sigma(p_{k+1,d} - p_{k,d}) = \Sigma \frac{1}{2} \rho \frac{f_{k-k+1,d} l_{k-k+1,d}}{D_{k-k+1,d}} \frac{Q_{k-k+1,d}^2}{A_{k-k+1,d}^2}$$
$$+ \rho l_{k-k+1,d} \frac{\dot{Q}_{k-k+1,d}}{\dot{A}_{k-k+1,d}} + \frac{1}{2} \rho \Sigma K_{k-k+1,d} \frac{Q_{k-k+1,d}^2}{A_{k-k+1,d}^2} + \rho g h_{k-k+1,d} \quad (3)$$

3.2 Forces and driving torque

3.2.1 Basic relationships

The parameters used to analyze the forces and driving torque of the rotary clap pump were defined previously.[1] That study found that the relative velocities between the two rotors make one rotor lead and lag periodically with respect to the other. Those lead and lag motions result

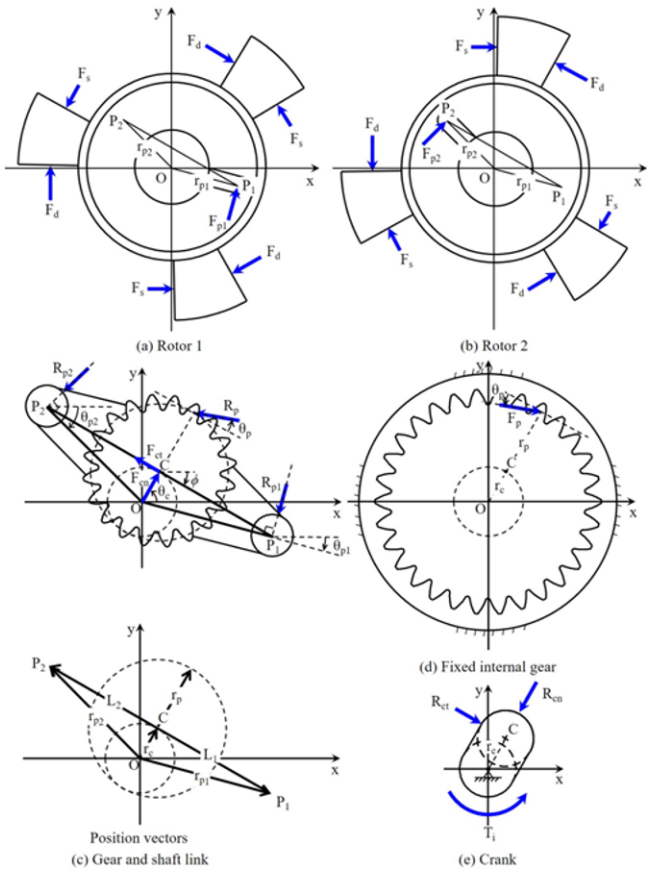

Fig. 7 Free body diagram of two rotors, gear, fixed internal gear, and crank

in a continuous cycle of approach-contact-recess between two adjacent rotor jaws. The continuous lead and lag motions produce the suction and discharge motions required for pumping. Suction and discharge pressures are generated by those motions between the two adjacent rotors and the rotor housing. Fig. 6 shows the hydraulic forces caused by the suction and discharge pressures, whose directions change periodically. Those forces are transmitted sequentially to the prime mover through each rotor, the gear, and the crank.

To simplify the force and driving torque analysis of each component, we neglected the friction losses that result from sliding conditions within the pump. The effect of the differential pressure, p_d - p_s, can now be considered as a uniformly distributed load in that plane. We analyzed the driving torque and forces of the main components using two-dimensional Cartesian coordinates because the axial forces are negligible.

Fig. 7 shows the free body diagram of the main components. In Figs. 7(a) and (b), the discharge forces, F_d, act on one side of each jaw at the same time that the suction forces, F_s, act on its other side. In addition, two forces, F_{p1} and F_{p2}, act on the pin slot joints of each rotor. The forces, F_{ct} and F_{cn} shown in Fig. 7(c) acting on the gear at point C, are the tangential and normal components, respectively, and the reaction forces, R_p, R_{p1}, and R_{p2}, act on the gear tooth and two pins, respectively. T_i is the driving torque required to maintain motion with the given conditions, and R_{ct} and R_{cn} are the reaction forces acting on the crank, as shown in Fig. 7(e). To analyze the forces of the components within the pump and driving torque, its position and force vectors are defined as Eqs. (4)~(14).

$$\mathbf{r}_c = (r_c\cos\theta_c, r_c\sin\theta_c) \tag{4}$$

$$\mathbf{r}_{p1} = (r_{p1}\cos\theta_{p1}, r_{p1}\sin\theta_{p1}) \tag{5}$$

$$\mathbf{r}_{p2} = (-r_{p2}\cos\theta_{p2}, -r_{p2}\sin\theta_{p2}) \tag{6}$$

$$\mathbf{r}_p = (r_p\cos\theta_c, r_p\sin\theta_c) \tag{7}$$

$$\mathbf{L}_1 = (r_{p1}\cos\theta_{p1} - r_c\cos\theta_c, r_{p1}\sin\theta_{p1} - r_c\sin\theta_c) \tag{8}$$

$$\mathbf{L}_2 = (-r_{p2}\cos\theta_{p2} - r_c\cos\theta_c, -r_{p2}\sin\theta_{p2} - r_c\sin\theta_c) \tag{9}$$

$$-\mathbf{F}_{p1} = \mathbf{R}_{p1} = \left(R_{p1}\cos\left(\theta_{p1} - \frac{\pi}{2}\right), R_{p1}\sin\left(\theta_{p1} - \frac{\pi}{2}\right)\right) \tag{10}$$

$$-\mathbf{F}_{p2} = \mathbf{R}_{p2} = \left(R_{p2}\cos\left(\theta_{p2} - \frac{\pi}{2}\right), R_{p2}\sin\left(\theta_{p2} - \frac{\pi}{2}\right)\right) \tag{11}$$

$$\mathbf{R}_p = \left(R_p\cos\left(\theta_c + \frac{\pi}{2} + \theta_p\right), R_p\sin\left(\theta_c + \frac{\pi}{2} + \theta_p\right)\right) \tag{12}$$

$$\mathbf{F}_{cn} = -\mathbf{R}_{cn} = (F_{cn}\cos\theta_c, F_{cn}\sin\theta_c) \tag{13}$$

$$\mathbf{F}_{ct} = -\mathbf{R}_{ct} = \left(F_{ct}\cos\left(\theta_c + \frac{\pi}{2}\right), F_{ct}\sin\left(\theta_c + \frac{\pi}{2}\right)\right) \tag{14}$$

3.2.2 Driving torque and forces analysis in rotary clap pump

The direction of the suction pressure, p_s, and discharging pressure, p_d, change periodically, as shown in Fig. 6. Thus the forces, F_{R1} and F_{R2}, of each rotor can be expressed as

$$-F_{R_1} = F_{R_2} = W_j hN(p_d - p_s) = N(F_d - F_s) \tag{15}$$

and the rotor torques about the center of rotation O, T_{OR1}, and T_{OR2} are

$$T_{OR_1} = -F_{R_1}\left(r_o + \frac{h}{2}\right) + F_{p1}r_{p1} = I_{R_1}\ddot{\theta}_{p1} \tag{16}$$

$$T_{OR_2} = -F_{R_2}\left(r_o + \frac{h}{2}\right) + F_{p2}r_{p2} = I_{R_2}\ddot{\theta}_{p2} \tag{17}$$

The angular velocities of the shaft link and gear are $\left(1 - \frac{Z_r}{Z_p}\right)\dot{\theta}_c$ when the angular velocity of the crank is θ_c[1]. In other words, the velocities of the shaft link and gear are kept constant. Therefore, the summation of the force vectors, $\Sigma \boldsymbol{F}_{sum}$, and torque vectors, $\Sigma \boldsymbol{T}_c$, acting on the gear and shaft link can be expressed as

$$\Sigma\mathbf{F}_{sum} = \mathbf{R}_{p1} + \mathbf{R}_{p2} + \mathbf{R}_p + \mathbf{F}_{cn} + \mathbf{F}_{ct} = 0 \tag{18}$$

$$\Sigma\mathbf{T}_c = \mathbf{L}_2 \times \mathbf{R}_{p2} + \mathbf{L}_1 \times \mathbf{R}_{p1} + \mathbf{r}_p \times \mathbf{R}_p = 0 \tag{19}$$

Converting the vectors of Eq. (19) into scalars and rearranging them gives

$$\begin{aligned} T_c = {} & (-r_{p2}\cos\theta_{p2} - r_c\cos\theta_c)R_{p2}\sin\left(\theta_{p2} - \frac{\pi}{2}\right) \\ & -(-r_{p2}\sin\theta_{p2} - r_c\sin\theta_c)R_{p2}\cos\left(\theta_{p2} - \frac{\pi}{2}\right) \\ & +(r_{p1}\cos\theta_{p1} - r_c\cos\theta_c)R_{p1}\sin\left(\theta_{p1} - \frac{\pi}{2}\right) \\ & -(r_{p1}\sin\theta_{p1} - r_c\sin\theta_c)R_{p1}\cos\left(\theta_{p1} - \frac{\pi}{2}\right) \\ & + r_p\cos\theta_c R_p\sin\left(\theta_c + \frac{\pi}{2} + \theta_p\right) - r_p\sin\theta_c R_p\cos\left(\theta_c + \frac{\pi}{2} + \theta_p\right) = 0 \end{aligned} \tag{20}$$

and rearranging for R_p gives

$$R_p = \frac{\left\{\begin{array}{l}\left(-r_{p_2}\cos\theta_{p_2} - r_c\cos\theta_c\right)R_{p_2}\sin\left(\theta_{p_2}-\frac{\pi}{2}\right)\\ -\left(-r_{p_2}\sin\theta_{p_2} - r_c\sin\theta_c\right)R_{p_2}\cos\left(\theta_{p_2}-\frac{\pi}{2}\right)\\ +\left(r_{p_1}\cos\theta_{p_1} - r_c\cos\theta_c\right)R_{p_1}\sin\left(\theta_{p_1}-\frac{\pi}{2}\right)\\ -\left(r_{p_1}\sin\theta_{p_1} - r_c\sin\theta_c\right)R_{p_1}\cos\left(\theta_{p_1}-\frac{\pi}{2}\right)\end{array}\right\}}{\left\{\begin{array}{l}-r_p\cos\theta_c\sin\left(\theta_c+\frac{\pi}{2}+\theta_p\right)\\ +r_p\sin\theta_c\cos\left(\theta_c+\frac{\pi}{2}+\theta_p\right)\end{array}\right\}} \tag{21}$$

Converting the vectors of Eq. (18) into scalars and separating the x axis and y axis yields,

$$\begin{aligned}\Sigma F_x &= R_{p1}\cos\left(\theta_{p1}-\frac{\pi}{2}\right)+R_{p2}\cos\left(\theta_{p2}-\frac{\pi}{2}\right)\\ &+R_p\cos\left(\theta_c+\frac{\pi}{2}+\theta_p\right)+F_{cn}\cos\theta_c+F_{ct}\cos\left(\theta_c+\frac{\pi}{2}\right)=0\end{aligned} \tag{22}$$

$$\begin{aligned}\Sigma F_y &= R_{p1}\sin\left(\theta_{p1}-\frac{\pi}{2}\right)+R_{p2}\sin\left(\theta_{p2}-\frac{\pi}{2}\right)\\ &+R_p\sin\left(\theta_c+\frac{\pi}{2}+\theta_p\right)+F_{cn}\sin\theta_c+F_{ct}\sin\left(\theta_c+\frac{\pi}{2}\right)=0\end{aligned} \tag{23}$$

Solving for F_{cn} and F_{ct} yields,

$$F_{ct} = \frac{\left\{\begin{array}{l}\sin\theta_c\left\{\begin{array}{l}R_{p_1}\cos\left(\theta_{p_1}-\frac{\pi}{2}\right)+R_{p_2}\cos\left(\theta_{p_2}-\frac{\pi}{2}\right)\\ +R_p\cos\left(\theta_c+\frac{\pi}{2}+\theta_p\right)\end{array}\right\}\\ -\cos\theta_c\left\{\begin{array}{l}R_{p_1}\sin\left(\theta_{p_1}-\frac{\pi}{2}\right)+R_{p_2}\sin\left(\theta_{p_2}-\frac{\pi}{2}\right)\\ +F_p\sin\left(\theta_c+\frac{\pi}{2}+\theta_p\right)\end{array}\right\}\end{array}\right\}}{\cos\theta_c\sin\left(\theta_c+\frac{\pi}{2}\right)-\sin\theta_c\cos\left(\theta_c+\frac{\pi}{2}\right)} \tag{24}$$

$$F_{cn} = \frac{\left\{\begin{array}{l}\sin\left(\theta_c+\frac{\pi}{2}\right)\left\{\begin{array}{l}R_{p_1}\cos\left(\theta_{p_1}-\frac{\pi}{2}\right)+R_{p_2}\cos\left(\theta_{p_2}-\frac{\pi}{2}\right)\\ +R_p\cos\left(\theta_c+\frac{\pi}{2}+\theta_p\right)\end{array}\right\}\\ -\cos\left(\theta_c+\frac{\pi}{2}\right)\left\{\begin{array}{l}R_{p_1}\sin\left(\theta_{p_1}-\frac{\pi}{2}\right)+R_{p_2}\sin\left(\theta_{p_2}-\frac{\pi}{2}\right)\\ +R_p\sin\left(\theta_c+\frac{\pi}{2}+\theta_p\right)\end{array}\right\}\end{array}\right\}}{\cos\left(\theta_c+\frac{\pi}{2}\right)\sin\theta_c-\sin\left(\theta_c+\frac{\pi}{2}\right)\cos\theta_c} \tag{25}$$

The reaction force from the crank, R_{ct}, is in the opposite direction to the force, F_{ct}. Therefore, the driving torque about point O gives,

$$T_i = r_c \times R_{ct} \tag{26}$$

Table 1 Parameters involved in the parametric study

Parameters	Values
$\Delta p = p_d - p_s$	0.5×10^6 N/m^2
r_c	5 mm
L	40 mm
W_j	50 mm
h	40 mm
r_o	65 mm
Z_r	30
Z_p	20
I_{R1}	0 kg·m^2
I_{R2}	0 kg·m^2

3.2.3 Parametric study

Table 1 gives the parameters of the rotary clap pump being used as an example to demonstrate the characteristics of the forces and driving torque. Because the direction of the hydraulic forces changes periodically, the forces of the two rotors alternate between positive and negative values, as shown in Fig. 8. Thus, the forces of the two pins change periodically, and there are some differences between the magnitudes of the forces of the two pins R_{p1}-R_{p2}, as shown in Fig. 9. That difference makes the pump rotate. As shown in Figs. 6, 10 and 11, the bending forces that act on the pair of gears of the shaft link and the driving torque are maximized when θ_{rel} is zero and zero when θ_{rel} is maximal or minimal.

The driving torque characteristics of the rotary clap pump vary with the crank radius, pin distance, number of jaws, jaw width, and height as shown in previous study,[1] and Eqs. (24) and (26). Fig. 12 shows the driving torque when the width and height of the jaw are kept constant. The driving torque increases with the crank radius for a given number of jaws and pin distance. However, at a given crank radius, it increases with the number of jaws and decreases with the pin distance. Because the crank radius is limited as the number of jaws increases, the available maximum driving torque is also limited according to the number of jaws. The characteristics of the pin forces are the same for different driving torques, as shown in Fig. 13. However, the gear forces are the only opposite result for a given crank radius and pin distance. The gear force decreases with the number of jaws.

We analyzed the driving torque, pin forces, and gear forces to determine the component size and driving torque input required for operation of the rotary clap pump. Based on the results, the crank radius should be minimized and the distance between two pins should be maximized to minimize the input power and forces acting on the components. In addition, the input power and pin forces could be minimized when the number of jaws was two. However, the gear forces showed an opposite trend, i.e., they are minimized when the number of jaws was five.

3.3 Efficiencies

3.3.1 Fundamental relationships

The displacement D is the volumetric flow rate per revolution of the shaft. Therefore, the volumetric flow rate Q_{vol} when the pump shaft speed is n *rad/s* is given by

$$Q_{vol} = \frac{D}{2\pi}n = D_p n \tag{27}$$

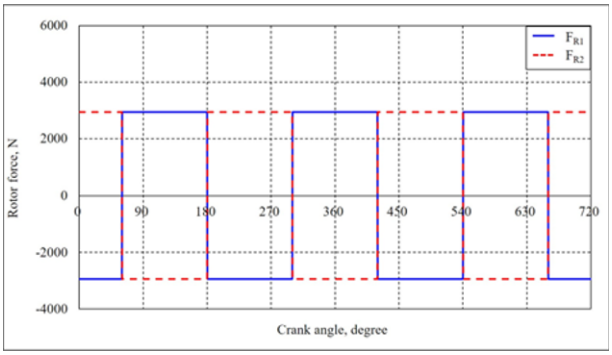

Fig. 8 Rotor forces F_{R1} and F_{R2} with crank angle

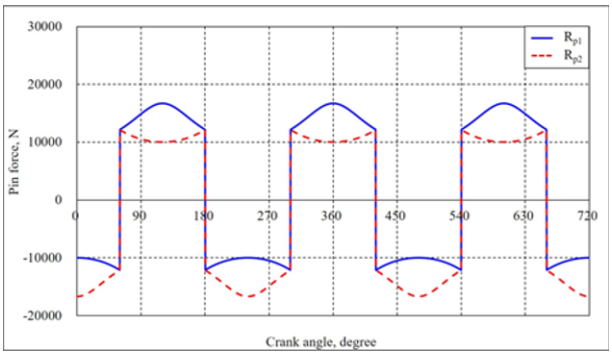

Fig. 9 Pin forces R_{p1} and R_{p2} with crank angle

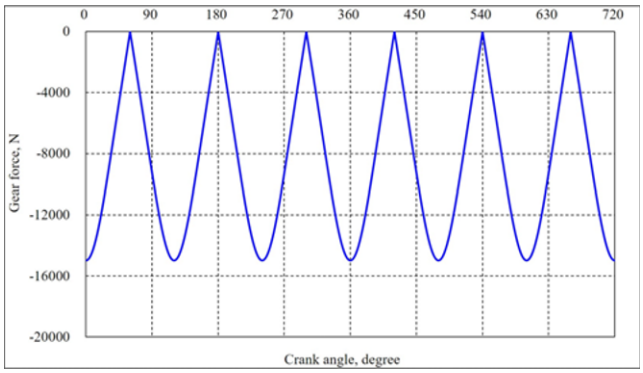

Fig. 10 Gear force R_p with crank angle

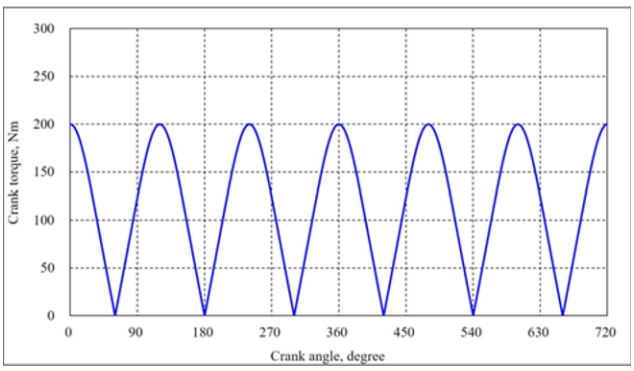

Fig. 11 Driving torque T_i with crank angle

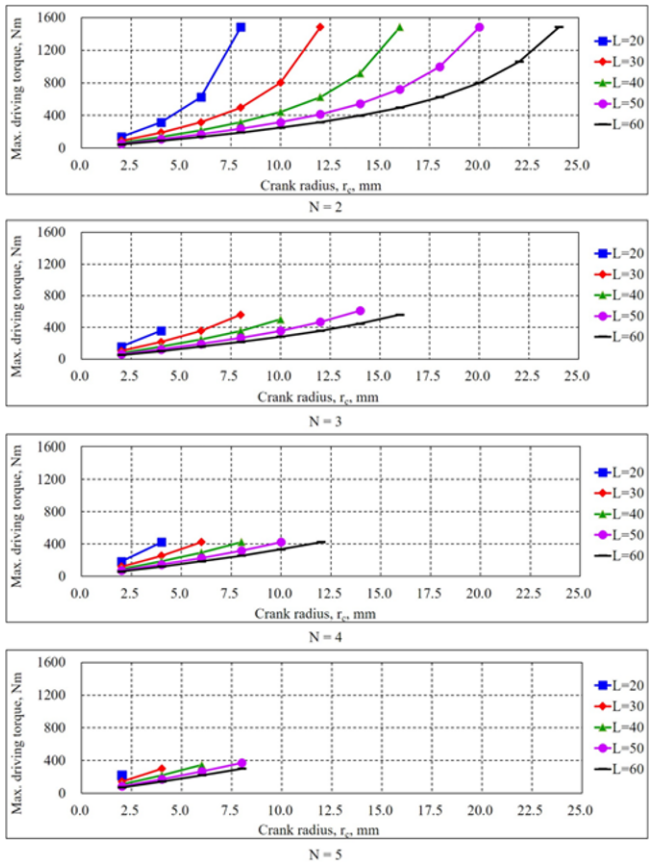

Fig. 12 Driving torque vs. crank radius

The ideal input power, for which the losses are neglected, is given by

$$T_{th}n = pQ_{vol} = pD_p n \tag{28}$$

From Eq. (28),

$$T_{th} = pD_p \tag{29}$$

However, in reality, torque losses and flow leakage take place when the pump is driving. The torque losses are represented by T_{loss}, and the flow leakage is represented by Q_s. Thus, the actual driving torque of the shaft and flow are given by

$$T = T_{th} + T_{loss} \tag{30}$$

$$Q = Q_{vol} - Q_s \tag{31}$$

Therefore, the volumetric efficiency, torque efficiency, and overall efficiency are defined as follows:

$$\eta_v = \frac{Q}{Q_{vol}} \tag{32}$$

$$\eta_t = \frac{T_{th}}{T} = \frac{D_p p}{T} \tag{33}$$

$$\eta = \frac{pQ}{Tn} = \frac{Q}{Q_{vol}}\frac{Q_{th}p}{Tn} = \frac{Q}{Q_{vol}}\frac{D_p p}{T} = \eta_v \eta_t \tag{34}$$

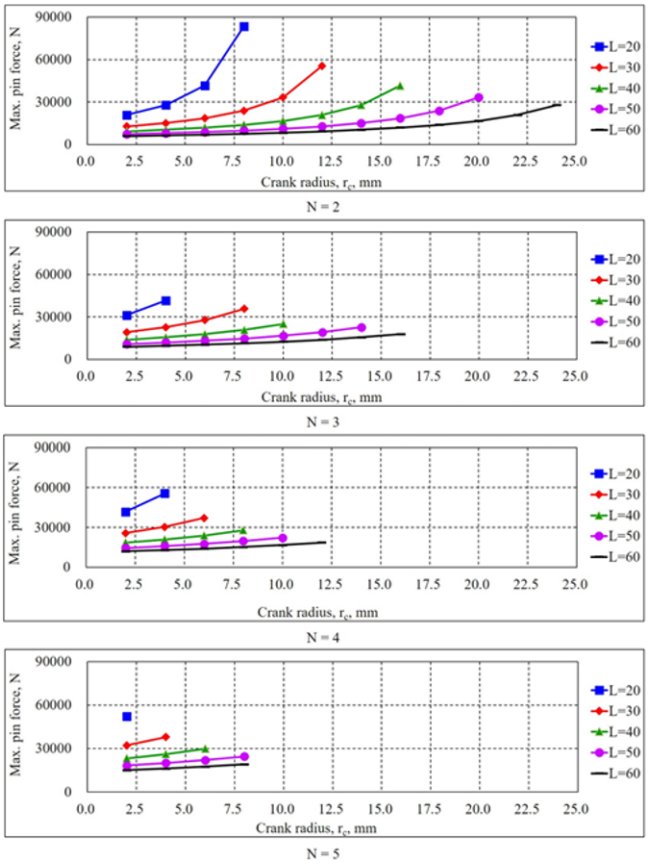

Fig. 13 Pin forces vs. crank radius

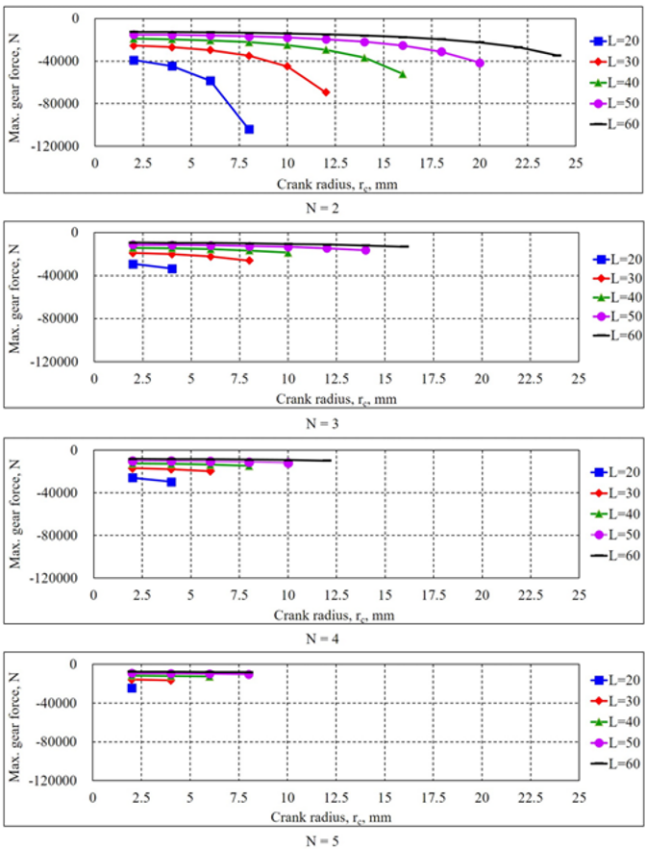

Fig. 14 Gear forces vs. crank radius

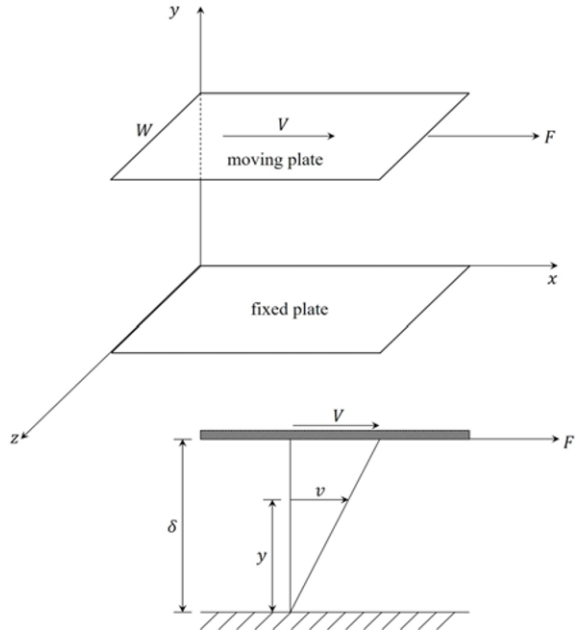

Fig. 15 Drag caused by the viscosity of the fluid[8]

3.3.2 General pump slip and forces caused by fluid viscosity

A positive-displacement pump needs a clearance between the rotating elements and the chamber to move the fluid. This makes it inevitable that some leakage will occur through the clearance, which is known as slip. Because slip affects the pump performance, it is important to quantify the total slip in the design and development of a pump.

The conventional method for analyzing pump slip uses Newton's law of viscosity. It is assumed that all of the flow in the pump is laminar and passes between moving and fixed flat plates (Fig. 15). Then, the shear stress caused by the fluid viscosity can be expressed as

$$\tau = \mu \frac{dv}{dy} \tag{35}$$

It is assumed that the pressure is constant throughout the fluid. Then, the total shear force acting on each plate surface parallel to these plates is given by

$$F = \tau A \tag{36}$$

To obtain the velocity of fluid v, Eq. (35) is integrated:

$$\begin{aligned} \int \tau dy &= \int \mu dv \\ \tau y &= \mu v + C \end{aligned} \tag{37}$$

Substituting the boundary conditions $v = V, y = \delta$ into Eq. (37) gives

$$v = V - \frac{\tau}{\mu}(\delta - y) \tag{38}$$

Fig. 16 shows a fluid with viscosity μ in a laminar and steady-state flow between parallel flat plates with the width W. The equation of equilibrium for a fluid element can be written as

$$pWdy - \left(p + \frac{dp}{dx}dx\right)Wdy + \left(\tau + \frac{d\tau}{dy}dy\right)Wdx - \tau Wdx = 0 \tag{39}$$

Integrating this and substituting it into Eq. (35) produces

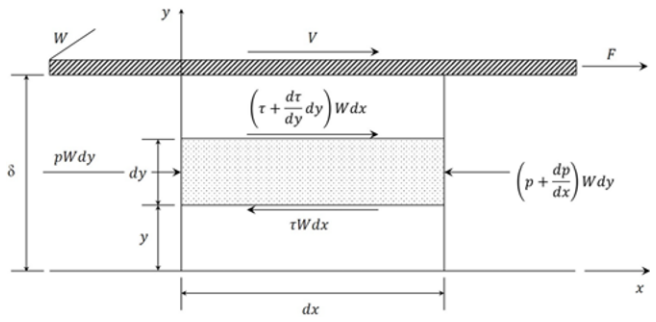

Fig. 16 Viscous and pressure forces acting on a fluid element[8]

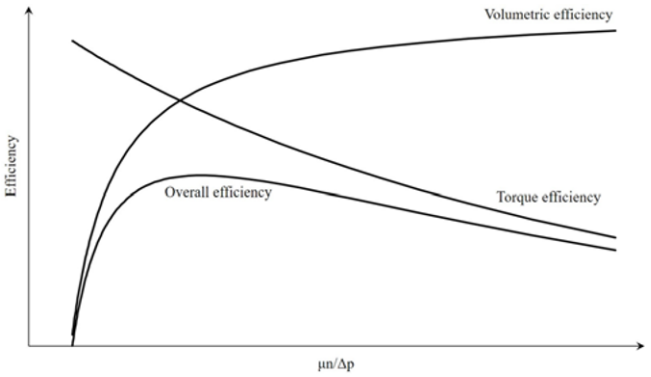

Fig. 17 Wilson's efficiency curve for a pump[8]

$$\mu\frac{dv}{dy}=\frac{dp}{dx}y+C_1 \tag{40}$$

Substituting the boundary conditions $y = 0$ at $v = 0$ and $y = \delta$ at $v = V$ into this equation after integration produces

$$v=\frac{Vy}{\delta}+\frac{1}{2\mu}\frac{dp}{dx}(y^2-y\delta) \tag{41}$$

Thus, the total flow between two plates can be expressed as

$$Q=\int v\,dA=\int_0^{\delta} vW\,dy=W\int_0^{\delta}\left[\frac{Vy}{\delta}+\frac{1}{2\mu}\frac{dp}{dx}(y^2-y\delta)\right]dy \tag{42}$$

Integration between the indicated limits gives

$$Q=\frac{VW\delta}{2}-\frac{W\delta^3}{12\mu}\frac{dp}{dx} \tag{43}$$

The total forces F_m acting on the moving plate and F_f acting on the fixed plate are given by

$$F_m=\tau_m lW \tag{44-a}$$

$$F_f=\tau_f lW \tag{44-b}$$

Then, the total forces can be expressed by

$$F_m=\left(\mu\frac{V}{\delta}+\frac{\delta}{2}\frac{dp}{dx}\right)lW \tag{45-a}$$

$$F_f=\left(\mu\frac{V}{\delta}-\frac{\delta}{2}\frac{dp}{dx}\right)lW \tag{45-b}$$

With those equations, if the distance to the axis of rotation is given by r, then the torque caused by the forces acting on this element is given by

$$T=F_m r=\left(\mu\frac{V}{\delta}+\frac{\delta}{2}\frac{dp}{dx}\right)lWr \tag{46}$$

3.3.3 Efficiency of conventional positive-displacement pump

The basic and representative method for evaluating the efficiency of a conventional positive-displacement pump uses Wilson's equation.[8] The slip flow is assumed to take place in the laminar range between parallel plates, and the viscosity is assumed to remain constant along the path of the flow. Under those assumptions and using Eq. (43), the effect of speed can be neglected. Thus, the slip flow of a conventional positive-displacement pump can be expressed as

$$\Delta Q_s=\frac{W\delta^3}{12\mu}\frac{\Delta p}{\Delta l} \tag{47}$$

From Eqs. (31) and (51), the total slip flow Q_s can be simplified as

$$Q_s=C_s D_p\frac{\Delta p}{\mu} \tag{48}$$

Therefore, the actual flow for the pump is given by

$$Q=Q_{vol}-C_s D_p\frac{\Delta p}{\mu} \tag{49}$$

From Eq. (32), the volumetric efficiency of the pump can be expressed as

$$\eta_v=\frac{Q}{Q_{vol}}=\frac{D_p n-C_s D_p\frac{\Delta p}{\mu}}{D_p n}=1-C_s\frac{\Delta p}{\mu n} \tag{50}$$

With the same method, the first term of Eq. (46) can be expressed as

$$T_v=C_d D_p\mu n \tag{51}$$

The second term of Eq. (46) is given by

$$T_f=C_f D_p\Delta p \tag{52}$$

Therefore, the total torque T can be represented as

$$T=T_{th}+T_v+T_f=\Delta p D_p+C_d D_p\mu n+C_f D_p\Delta p \tag{53}$$

From Eq. (33), the torque efficiency of the pump can be expressed as

$$\eta_t=\frac{T_{th}}{T}=\frac{1}{1+\left(C_d\frac{\mu n}{\Delta p}+C_f\right)} \tag{54}$$

The overall efficiency is given by

$$\eta=\frac{1-C_s\frac{\Delta p}{\mu n}}{1+C_d\frac{\mu n}{\Delta p}+C_f} \tag{55}$$

All of the efficiencies can be represented as a function of $\mu n/\Delta p$, as shown in Fig. 17.

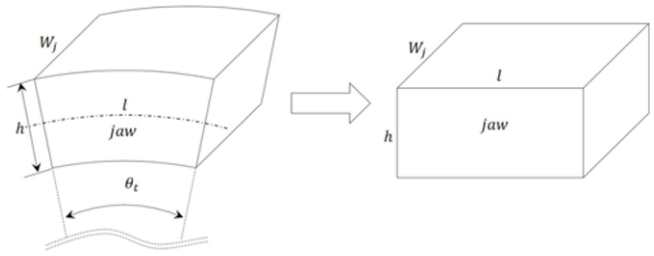

Fig. 18 Jaw model simplified as a rectangle for the analysis of flow and torque losses

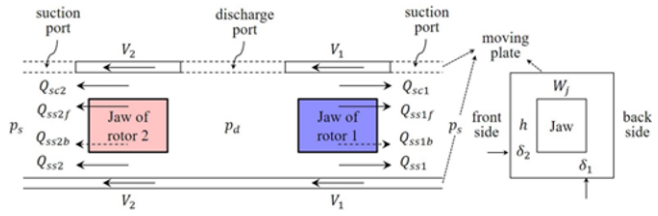

Fig. 19 Flow losses in suction and discharge chambers of the pump

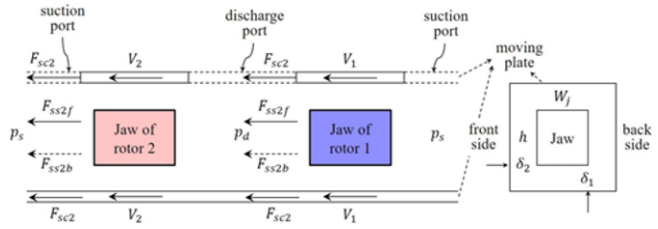

Fig. 20 Force losses in suction and discharge chambers of the pump

3.3.4 Slip and forces caused by fluid viscosity in rotary clap pump

To apply that performance theory to this pump, we simplified the rotor jaws into parallel flat plates, as shown in Fig. 18. The slip flow and forces caused by the fluid viscosity in the suction and discharge chamber can be expressed as shown in Figs. 19 and 20, respectively.

As presented in previous study[1] and Fig. 6, the direction of the suction and discharge pressures p_s and p_d change periodically because of the lead-lag motion of the rotors. Therefore, when $V_1 \geq V_2$, d_p/d_x in Eqs. (43), (45), and (46) have a positive value. When $V_1 < V_2$, d_p/d_x have a negative value. The velocities of V_1 and V_2 are given by

$$V_1 = \dot{\theta}_{p1} \times \left(r_o + \frac{h}{2} \right) \tag{56-a}$$

$$V_2 = \dot{\theta}_{p2} \times \left(r_o + \frac{h}{2} \right) \tag{56-b}$$

Because the velocities V_1 and V_2 vary periodically as given in Eqs. (22), (24), and (56) and the pump has several ports for suction and discharge, the first term of Eq. (43) cannot be neglected for this pump. Therefore, the total slip flow and forces caused by fluid viscosity in the suction and discharge chambers are given as follows:

1) $V_1 \geq V_2$

$$(Q_{sc1})_{tot} = 2N\left\{ \frac{V_1 W_j \delta_1}{2} - \frac{W_j \delta_1^3 p_s - p_d}{12\mu \quad l} \right\} \tag{57-a}$$

$$(Q_{ss1})_{tot} = Q_{ss1f} + Q_{ss1b} = 2N\left\{ \frac{V_1 h \delta_2}{2} - \frac{h \delta_2^3 p_s - p_d}{12\mu \quad l} \right\} \tag{57-b}$$

$$(Q_{sc2})_{tot} = 2N\left\{ \frac{V_2 W_j \delta_1}{2} - \frac{W_j \delta_1^3 p_s - p_d}{12\mu \quad l} \right\} \tag{57-c}$$

$$(Q_{ss2})_{tot} = -(Q_{ss2f} + Q_{ss2b}) = -2N\left\{ \frac{V_2 h \delta_2}{2} - \frac{h \delta_2^3 p_s - p_d}{12\mu \quad l} \right\} \tag{57-d}$$

2) $V_1 < V_2$

$$(Q_{sc1})_{tot} = -2N\left\{ \frac{V_1 W_j \delta_1}{2} - \frac{W_j \delta_1^3 p_s - p_d}{12\mu \quad l} \right\} \tag{57-e}$$

$$(Q_{ss1})_{tot} = -2N\left\{ \frac{V_1 h \delta_2}{2} - \frac{h \delta_2^3 p_s - p_d}{12\mu \quad l} \right\} \tag{57-f}$$

$$(Q_{sc2})_{tot} = 2N\left\{ \frac{V_2 W_j \delta_1}{2} - \frac{W_j \delta_1^3 p_s - p_d}{12\mu \quad l} \right\} \tag{57-g}$$

$$(Q_{ss2})_{tot} = 2N\left\{ \frac{V_2 h \delta_2}{2} - \frac{h \delta_2^3 p_s - p_d}{12\mu \quad l} \right\} \tag{57-h}$$

$$(Q_s)_{tot} = (Q_{sc1})_{tot} + (Q_{ss1})_{tot} + (Q_{sc2})_{tot} + (Q_{ss2})_{tot} \tag{57-i}$$

1) $V_1 \geq V_2$

$$(F'_{sc1})_{tot} = 2N\left\{ \mu \frac{V_1}{\delta_1} - \frac{\delta_1 p_s - p_d}{2 \quad l} \right\} l W_j \tag{58-a}$$

$$(F'_{ss1})_{tot} = F'_{ss1f} + F'_{ss1b} = 2N\left\{ \mu \frac{V_1}{\delta_2} - \frac{\delta_2 p_s - p_d}{2 \quad l} \right\} l h \tag{58-b}$$

$$(F'_{sc2})_{tot} = 2N\left\{ \mu \frac{V_2}{\delta_1} - \frac{\delta_1 p_s - p_d}{2 \quad l} \right\} l W_j \tag{58-c}$$

$$(F'_{ss2})_{tot} = 2N\left\{ \mu \frac{V_2}{\delta_2} - \frac{\delta_2 p_s - p_d}{2 \quad l} \right\} l h \tag{58-d}$$

2) $V_1 < V_2$

$$(F'_{sc1})_{tot} = 2N\left\{ \mu \frac{V_1}{\delta_1} - \frac{\delta_1 p_s - p_d}{2 \quad l} \right\} l W_j \tag{58-e}$$

$$(F'_{ss1})_{tot} = 2N\left\{ \mu \frac{V_1}{\delta_2} - \frac{\delta_2 p_s - p_d}{2 \quad l} \right\} l h \tag{58-f}$$

$$(F'_{sc2})_{tot} = 2N\left\{ \mu \frac{V_2}{\delta_1} - \frac{\delta_1 p_s - p_d}{2 \quad l} \right\} l W_j \tag{58-g}$$

$$(F'_{ss2})_{tot} = 2N\left\{ \mu \frac{V_2}{\delta_2} - \frac{\delta_2 p_s - p_d}{2 \quad l} \right\} l h \tag{58-h}$$

$$(F'_{slip})_{tot} = (F'_{sc1})_{tot} + (F'_{ss1})_{tot} + (F'_{sc2})_{tot} + (F'_{ss2})_{tot} \quad (58\text{-i})$$

3.3.5 Efficiency analysis in rotary clap pump

The efficiencies of the rotary clap pump can be obtained using Eqs. (50), (54), and (55). From Eq. (39) in previous study,[1] Eqs. (50), and (57), the volumetric efficiency is given by

$$\eta_v = \frac{Q_{vol} - (Q_s)_{tot}}{Q_{vol}} \quad (59)$$

The forces $(F"_{slip})_{tot}$ caused by the fluid viscosity increase the forces acting on each rotor. Therefore, the total torque T can be obtained by substituting $-F_{R1}+(F"_{sc1})_{tot}+(F"_{ss1})_{tot}$ and $F_{R2}+(F"_{sc2})_{tot}+(F"_{ss2})_{tot}$ into Eq. (15). From Eqs. (4) – (26) and (58), the torque efficiency is then given by

$$\eta_t = \frac{T_i}{T} \quad (60)$$

The overall efficiency is given by

$$\eta = \eta_v \times \eta_t = \frac{Q_{vol} - (Q_s)_{tot}}{Q_{vol}} \times \frac{T_i}{T} \quad (61)$$

4. Conclusions

In this study, we have analyzed the pump performance of the rotary clap pump that was developed to increase its displacement with less vibration and power loss. The considered performance parameters were pressure, driving torque, and efficiency. In the pressure analysis, the effect of friction, mass acceleration, piping components, and gravity were considered. The forces acting on the pump components and the driving torque were calculated using vector equations based on the results of previous study. We analyzed the volumetric, torque, and overall efficiencies by calculating the slip flow and frictional forces caused by fluid viscosity.

We divided the suction and discharge spaces in the pump into five independent control volumes and then simplified the spaces to circular pipes to analyze the pressure of the pump. Because the axial forces were negligible, we calculated the driving torque and forces of the main components using two-dimensional Cartesian coordinates. Based on the analysis, we found that the crank radius should be minimized and the distance between two pins should be maximized to minimize the input power and forces acting on the components. In addition, the input power and pin forces can be minimized when the number of jaws is two. However, the gear force showed the opposite trend. We analyzed the slip flow and viscous forces of the pump using the conventional method based on Newton's law of viscosity. Because the suction and discharge pressure change periodically with the lead-lag motion of the rotors and because the pump has several ports for suction and discharge, the velocity term of the equations for the slip flow and viscous forces could not be neglected for this pump. We evaluated the efficiencies of the rotary clap pump by Wilson's equation using the slip flow and viscous forces.

ACKNOWLEDGEMENT

This work was supported by Korea Institute of Planning and Evaluation for Technology in Food, Agriculture, Forestry and Fisheries (IPET) through Agriculture, Food and Rural Affairs Research Center Support Program, funded by Ministry of Agriculture, Food and Rural Affairs (MAFRA) (716001-7).

REFERENCES

1. Shim, S. B., Park, Y. J., Kim, J. M., and Kim, K. U., "Development of a Rotary Clap Mechanism for Positive-Displacement Rotary Pumps: Kinematic Analysis and Working Principle," Journal of Mechanical Science and Technology, Vol. 29, No. 2, pp. 759-767, 2015.
2. Corbo, M. A. and Stearns, C. F., "Practical Design against Pump Pulsations," Proc. of the 22nd International Pump Users Symposium, pp. 137-177, 2005.
3. Manring, N. D., "Measuring Pump Efficiency: Uncertainty Considerations," Journal of Energy Resources Technology, Vol. 127, No. 4, pp. 280-284, 2005.
4. Manring, N., "The Torque on the Input Shaft of an Axial-Piston Swash-Plate Type Hydrostatic Pump," Transactions-American Society of Mechanical Engineers Journal of Dynamic Systems Measurement and Control, Vol. 120, No. 1, pp. 57-62, 1998.
5. Schlucker, E., Blanding, J. M., and Murray, J., "Guidelines to Maximize Reliability and Minimize Risk in Plants Using High Pressure Process Diaphragm Pumps," Proceedings of the International Pump Users Symposium, pp. 77-100, 1999.
6. Vetter, G. and Seidl, B., "Pressure Pulsation Dampening Methods for Reciprocating Pumps," Proc. of the 10th International Pump Users Symposium, pp. 25-40, 1993.
7. Schlücker, E., Fritsch, H., Stritzelberger, M., and Schwarz, J., "A New Evaluation Method for Estimating NPSH-Values of Reciprocating Positive Displacement Pumps," Proc. of ASME Fluids Engineering Division Summer Meeting, 1997.
8. Wilson, W. E., "Positive-Displacement Pumps and Fluid Motors," Pitman Publishing Corporation, 1950.